STATISTICS, OPTIMIZATION AND INFORMATION COMPUTING
Stat., Optim. Inf. Comput., Vol. **16**, November 2026, pp 3962–3976.
Published online in International Academic Press (www.IAPress.org)

An integrated performance, energy, and QoS evaluation of traffic-aware 5G mmWave small-cell networks under realistic urban assumptions

Sazan K. Al-Jaff*, Hussain A. Hammas, Zaid Ali Hamid, Halah I. Khani, and Mustafa Ghanim

University of Technology, Baghdad, Iraq
sazan.k.hasan@uotechnology.edu.iq, hussain.a.hammas@uotechnology.edu.iq,
zaid.a.hamid@uotechnology.edu.iq, halah.i.khani@uotechnology.edu.iq,
mustafa.g.rzooki@uotechnology.edu.iq

Abstract The extraordinary and rapid growth in mobile service demand has resulted in increasingly dense base station deployments across cellular communication generations from 2G to 5G. Although base station densification improves cellular networks capacity, it also introduces significant energy consumption, extra infrastructure, and increasing operational costs. This paper presents a framework for intelligent base station reduction that integrates realistic path loss models, and time-varying traffic control. Unlike traditional fixed-radius planning, we apply Free Space and COST-231 Hata propagation models to determine coverage feasibility, enabling accurate estimation of the required number of base station under both ideal and urban conditions. An adaptive algorithm is used to iteratively select base station sites based on residual traffic demand and signal attenuation. A dynamic switching control is implemented to deactivate underutilized base stations during low-traffic and enhancing energy efficiency.

Keywords 5G, millimeter wave, small cells, energy efficiency, beamforming, traffic-aware networks

DOI: 10.19139/soic-2310-5070-4284

1. Introduction

Mobile phones which were considered as luxury have now become an essential communication tool due to its necessity of our daily life. The exponential expansion in mobile data demand over the last decades has led to significant evolution in cellular mobile networks, from 2G voice systems to the high-capacity architectures of 5G [1, 2, 3].

Cellular mobile networks include the individual cell phones and the base stations which enable two-way radio wireless communication between subscribers and the core network. In 2G and 3G networks, the deployments of macrocells were sufficient to provide the required quality of service wide coverage areas. However, 5G networks depend heavily on higher frequency bands (including mmWave), and beamforming technologies [4]. While adoption of millimeter-wave frequency bands in 5G cellular networks enables high data rates through large bandwidths, it suffers from severe path loss, necessitating dense small-cell with higher dense base station deployments in urban environments. Efficient network design and energy consumption management have become critical challenges [5, 6, 7].

Each generation has brought improvements in spectral efficiency, data rate transmission, and latency. These improvements have driven significant increase in base station density, particularly in densely populated urban areas in close proximity to residential buildings, and commercial areas, to meet the increasing demand for higher capacity and coverage [8]. While base stations densification is beneficial and critical for ensuring high quality service and reliable connectivity, it has introduced new challenges related to [9, 10]:

*Correspondence to: Sazan K. Al-Jaff (Email: sazan.k.hasan@uotechnology.edu.iq). University of Technology, Baghdad, Iraq.

ISSN 2310-5070 (online) ISSN 2311-004X (print)
Copyright © 2026 International Academic Press

1. Energy consumption, as base stations account for 60–75% of the total network energy consumption.
2. Significant increase in operational expenditure costs.
3. Underutilized base stations during off-peak hours.
4. Significant increase in radio frequency (RF) pollution and visual pollution.

These challenges have driven interest in base station reduction strategies, to minimize the number of active base stations while managing their operational states with maintaining system coverage and quality of service (QoS).
Work by Trabelsi et al. (2024) showed that the cellular network performance improvements require denser deployment of base stations. This results in significant and unsustainable increase in the network's energy consumption. The study considered the sleep control (SC), for greener and more energy-efficient as this approach allows turning off some base station hardware components during low-traffic time and can be optimized through employment of Deep Reinforcement Learning [11].
A study conducted by Sare et al. (2024) [12] showed that utilization of cell-free massive multiple-input multiple-output (CF-MIMO) system may lead to high power consumption due to the large numbers of distributed access points. They suggested using the access pointed selection technique in a modified algorithm to improve overall energy efficiency and reduced the total power consumption.
A comprehensive review of reconfigurable intelligent surfaces (RIS) technology was presented by Prasetyo et al. (2025). They conclude that deployment of RIS in controlling the propagation environment and reflecting signals around obstacles may reduce the need of additional base stations [13].
The study introduced by Edward J. Oughton1 (2025) suggest infrastructure sharing strategies, as an effective approach for energy consumption and CO2 emissions reduction. Additionally, large financial cost reductions are possible in combination with other strategies [14]. Practical 5G deployments require an efficient evaluation that jointly considers coverage, capacity, and energy consumption under realistic traffic demand conditions. The static network dimensioning is usually based on peak demand leading to excessive energy consumption during off-peak hours [15].
This paper explores the concept of base station reduction through different approaches such as network densification with small cells, management, antenna beamforming, and adaptive power control to enable energy and spectrum efficient base station deployment. The paper uniquely integrates tri-objective optimization in a single, unified framework which represents highly valuable for network operation in real environment. Unlike prior work, the research integrates the network performance, energy consumption, and QoS under real urban assumptions such as non-uniform traffic, dynamic blockages, and street canyons. With standardized channel models, we quantify the trade-off between energy savings and QoS violations to provide cost-efficient and green cells by simple solutions without degrading user experience in dense scenarios.

2. Current and Future Wireless Networks

Fifth generation (5G) mobile networks fundamentally differ from traditional early-generation networks that depend primarily on static and wide-area macrocell deployments Figure 1 illustrates that an urban area in early networks is provided with a single macro high power base-station to overcome large radio signal path loss. Base station antennas are usually fixed on tall tower that may be located far from the users, increasing the cell phone battery draw on uplink [8]. However, in fifth generation (5G) networks, the same area can equivalently be served with smaller multiple low-power base-stations, that can be located closer to users at lower heights, which has positive effect on cell phone battery life as well [14].
5G networks adopt multi-band, where sub-6 GHz frequencies ensure coverage and mmWave frequencies to enable high data rates (capacity). The adoption of the frequency bands of the mm waves in fifth generation (5G), and the frequency band above 100GHz of sixth generation (6G) in the next few years, will result in higher densification of cellular networks and dense small-cell architectures that contribute significantly in energy consumption [8].
The power consumption of current and future mobile communication networks make energy efficiency to be critical design objective and new challenge regarding power consumption. The reduction of base station density and energy

consumption has become a critical research focus across successive generations of cellular networks, particularly in response to the growing operational costs, carbon footprint, and underutilization during off-peak periods.

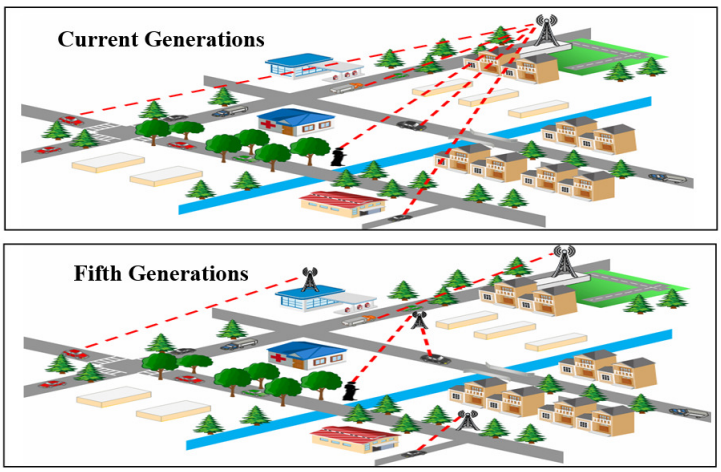

Figure 1. Early and fifth generation networks.

3. Theoretical Foundations of Base Stations Reduction

The optimization strategies of cellular mobile base stations deployment in all communication networks depend on balancing between the main network requirements (coverage, capacity, and interference) through quantitative systematic theoretical models. Integration all of these relationships into a unified optimization problem to meet target threshold of the quality of service (QoS) is very important to establish a theoretical model for minimizing the number of base stations.
This section derives the core equations governing base station reduction, beginning with propagation models that are helpful in cell sizes determination, followed by traffic and capacity limits and interference constraints.

3.1. Problem Formulation

The main objective is to minimize the number of base stations while ensuring coverage, capacity, and quality of service (QoS). Minimizing the number of base stations required ensuring that all users receive minimum signal strength (coverage), to meet the traffic demand by all users (capacity), and to satisfy the target SINR (QoS). Therefore, minimizing (NBS) must ensure that [8, 16]:

$$\begin{cases} P_i \geq P_{\min} & \text{(Coverage)} \\ \sum_i C_i \geq C_{\text{total}} & \text{(Capacity)} \\ \text{SINR} \geq \gamma_{\text{target}} & \text{(QoS)} \end{cases} \tag{1}$$

where N_{BS} is the number of base stations, P_r is the received power, $P_{\min}$ is the minimum required power, C_i is the capacity required by user i within the network, C_{total} is the total capacity, SINR is the signal-to-interference-plus-noise ratio, and γ_{target} is the network SINR threshold.

3.2. Coverage Modeling

The number of base stations in cellular mobile networks depends on cell coverage area, which can be predicated through path loss propagation models. Path loss prediction enables designer to estimate radio signal attenuation

over distance and the cell size (radius). For ideal line-of-sight (LoS) free space conditions, the path loss (P_L) is given as:

$$P_L(d) = 20\log_{10}(d) + 20\log_{10}(f) + 20\log_{10}\left(\frac{4\pi}{c}\right) \tag{2}$$

Where d is the T-R separation distance (m), f is the operating frequency (Hz), and c is the speed of light (3×10^8 m/s).
For Non-Line-of-Sight (NLOS), Okumura-Hata empirical radio wave propagation model can be applied for urban macro cells operating at 150–1500 MHz [5, 6]:

$$\begin{aligned} P_L(d) = 69.55 + 26.16\log_{10}(f) - 13.82\log_{10}(h_b) \\ - a(h_m) + (44.9 - 6.55\log_{10}(h_b))\log_{10}(d) \end{aligned} \tag{3}$$

Where h_b is the base station height (m), h_m is the mobile antenna height (m), and $a(h_m)$ is the correction factor for mobile height.
In COST-231 Hata Model that is extended to 2 GHz the path loss is given as [4]:

$$P_L(d) = [P_L(d)]_{\text{Hata}} + 3.0 \text{ dB} \tag{4}$$

The 3GPP UMi path loss model can be used for 5G networks. It is expressed as:

$$P_L(d) = 32.4 + 21\log_{10}(d) + 20\log_{10}(f_{\text{GHz}}) \tag{5}$$

$$P_r(d) = P_t + G_t + G_r - P_L(d) - \text{Margin} \geq P_{\min} \tag{6}$$

Where d is the T-R distance in meters, f is the operating frequency in GHz, P_t is the transmitted power, P_r is the received power, G_t and G_r are transmit and receive antenna gains respectively.
The maximum cell radius R_c can be derived from the maximum allowable path loss P_L by solving the path loss equations for d based on transmit power P_t, and the receiver sensitivity P_r [17]:

$$[P_L(d)]_{\max} = P_t + G_t + G_r - P_r - \text{Margin} \tag{7}$$

The cell radius R_c depends on transmit power P_t, path loss and the minimum required received power.
The radio signal propagation mechanism for 5G mmWave is dominated by diffraction and scattering/reflection, therefore, simple path-loss models are insufficient for the NLOS (Non-Line-of-Sight) propagation modeling. For urban NLOS at 28 GHz, the industry standard model that captures the urban canyon geometry 3GPP TR 38.901 UMi is employed. The model for a typical urban grid is expressed as [18]:

$$P_L(d)_{\text{NLoS}} = 32.4 + 31.9\log_{10}(d_{3D}) + 20\log_{10}\left(\frac{f}{10^9}\right) \tag{8}$$

Where f is the frequency in GHz, d_{3D} is the 3D distance between the base station and the user.in meters.
The NLOS model can be combined with the effect of interference from six neighboring cells at the first tier of a hexagonal cellular layout adjusting to the target cell. Additionally, building penetration loss for NLOS (15–25 dB for concrete), can be added to modify the model.
From the given path loss model, it can be concluded that higher base station antennas can cover larger areas, and then reduce the need for more base stations. The cell coverage area can be extended through using directional antennas with higher gain. The proper down tilt of the base station antenna can result in coverage improvement and interference reduction, allowing fewer sites to serve more users [19, 20].
The coverage per base station depends on cell radius R_c. For the circular shape cells, the cell area (A_{cell}) is given as

$$A_{\text{cell}} = \pi R_c^2 \tag{9}$$

If the entire network coverage area A_{total} is to be covered:

$$N_{\text{BS}} \geq \frac{A_{\text{total}}}{\pi R_c^2} \tag{10}$$

Assuming circular shape cells, the number of base stations (N_{BS}) in a total coverage area (A_{total}) can be given as [6]:

$$N_{\text{BS}} = \frac{A_{\text{total}}}{\pi R_c^2} \tag{11}$$

$$N_{\text{BS}} = \frac{A_{\text{total}}}{2.59 R_c^2} \tag{12}$$

3.3. Traffic Modeling

The number of base stations depends on traffic load. The Erlang-B formula determines the traffic intensity (A) in Erlangs for a given number of channels (C) and at a certain blocking probability [5, 6]:

$$P_b = \frac{\frac{A^C}{C!}}{\sum_{k=0}^{C} \frac{A^k}{k!}} \tag{13}$$

The goal of using the traffic model is to minimize the blocking probability (P_b) and reduce the number of cells. The traffic demand per each base station (T_{BS}) depends on user's density [6, 21]:

$$T_{\text{BS}} = \lambda \times \left(2.59 R_c^2\right) \times T_U \tag{14}$$

Where λ is the users density (number of users per km^2), and T_U is the average data rated required per each user in Mbps.
Each base station must handle total user traffic T, so:

$$N_{\text{BS}} \geq \frac{T_{\text{total}}}{T_{\text{BS}}} \tag{15}$$

$$T_{\text{total}} = U \times A_{\text{total}} \times T_U \tag{16}$$

$$N_{\text{BS}} \geq \frac{U \times A_{\text{total}} \times T_U}{T_{\text{BS}}} \tag{17}$$

The required number of base stations depends on user density (λ, users/km^2) and spectral efficiency (η, bps/Hz):

$$T_{\text{total}} = N_{\text{BS}} \times B \times \eta \geq \lambda \times A_{\text{total}} \times T_U \tag{18}$$

Increasing the average data rate per base station can be carried out via massive MIMO, and beamforming.

3.4. Capacity Modeling

Using Erlang-B and Shannon capacity can provide sufficient channels in a network. The capacity of a base station is limited by the Shannon-Hartley theorem [21]:

$$C = B \log_2(1 + \text{SINR}) \tag{19}$$

Where C is the capacity in bps (bits per second), B is the bandwidth (Hz), and SINR is Signal-to-Interference-plus-Noise Ratio.
Increasing the SINR ratio through interference management or using higher bandwidth can contribute in reduction of base stations number.

3.5. Dynamic Base Station Use

Introducing ON/OFF control for base stations operation based on time-of-day traffic patterns can be employed for energy efficiency optimization:

$$N_{\mathrm{BS}}(t) = \frac{U(t) \times A_{\mathrm{total}} \times T_U(t)}{T_{\mathrm{BS}}} \tag{20}$$

Then minimize average number of base stations used:

$$\min \frac{1}{T} \int_0^T N_{\mathrm{BS}}(t)\, dt \tag{21}$$

At all times, users Quality of Service (QoS), and coverage requirements can be achieved.

3.6. Interference Modeling

The received signal power at the receive antenna of the user unit placed at distance R_c from the serving base station is proportional to $(R_c)^{-\gamma}$, where (γ) is the path loss exponent value. There are six interfering cells surrounding the target cell as illustrated in Figure 2. Each lies at a distance (D_i), therefore the Signal to interference raio (SIR) can be given as [5]:

$$\frac{S}{I} = \frac{R_c^{-\gamma}}{\sum_{k=1}^{6} D_k^{-\gamma}} \tag{22}$$

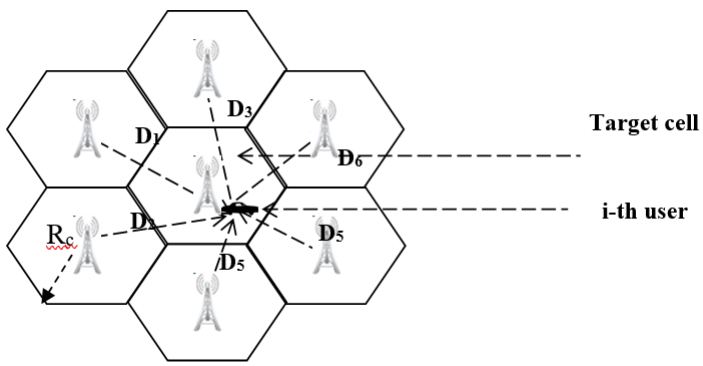

Figure 2. Interference due to surrounding cells.

4. Model Simulations

Simulation of the theoretical approach presented in the previous section requires combining all constraints regarding coverage, capacity, interference, and optimization frameworks to integrate all these requirements, while minimizing the number of base stations in wireless networks. The simulation will be carried out with the use of MATLAB.

The simulation is carried out with dynamic user traffic, and adaptive base station switching. The simulation steps are shown in the flowchart below.

4.1. Simulation of 3.5 GHz

An area of 2.0 km^2 is assumed with 100 users per km^2, and each user is assumed to generate a traffic intensity of 0.02 Erlang. The power transmitted by each base station, allocated bandwidth, QoS and path loss parameters are all shown in table 1 below.

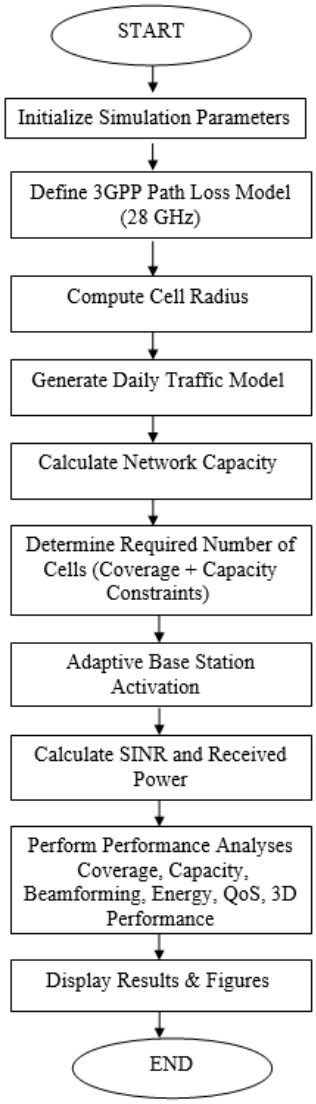

Table 1. Network Parameters

Base Stations		**Subscriber Units**	
Transmitted power P_t	40 dBm		
Antenna gain	10 dB	Antenna gain	2.0 dB
Allocated Bandwidth	20 MHz	Traffic Intensity	0.02 Erlang
Antennas type	Omni/sectored		
QoS parameters		**Path loss parameters**	
Minimum P_r	-90 dBm	Frequency	3.5 GHz
SINR Target	10 dB	LOS Path loss exponent	2.1
Blocking Probability	1%	NLOS Path loss exponent	3.0
Capacity per user	1.0 Mbps	Reference distance (d_0)	1.0 m

From Fig.3-a, it can be noticed that omni-directional antennas show SINR degradation below 0 dB when the number of base stations number is less than 10, indicating unsuitable for dense deployments. Three sectored base station maintains SINR more than 5.0 dB for up to 30 base stations, meeting minimum SINR for voice calls requirement. Additionally, base station provided with six sectored configurations can give higher SINR with 25 base stations, supporting video streaming. It can be concluded the number of base station or the optimal base station density depends on base station antennas configuration. Sectorization can improve SINR by 6–12 dB over omni-directional antennas, enabling higher base station density while maintaining QoS.
The Relationship between the capacity and SINR is plotted in Fig3-b. It can be noticed that the capacity growth follows logarithmic trend. Increasing SINR by 3 dB yields 10 Mbps. Increasing SINR in 10–15 dB range provides optimal balance between power consumption and achieved capacity. The network optimal operation in the 10–15 dB range is the best for power-efficient deployment.
Fig.3-c shows that high user density (> 200 users/km^2) with low number of base stations (< 15) cannot match the required SINR and capacity constraints, while more than 20 base stations can support up to 300 users/km^2 with acceptable SINR, and through 25 base stations the optimal balance, and the required SINR and capacity targets can be met.

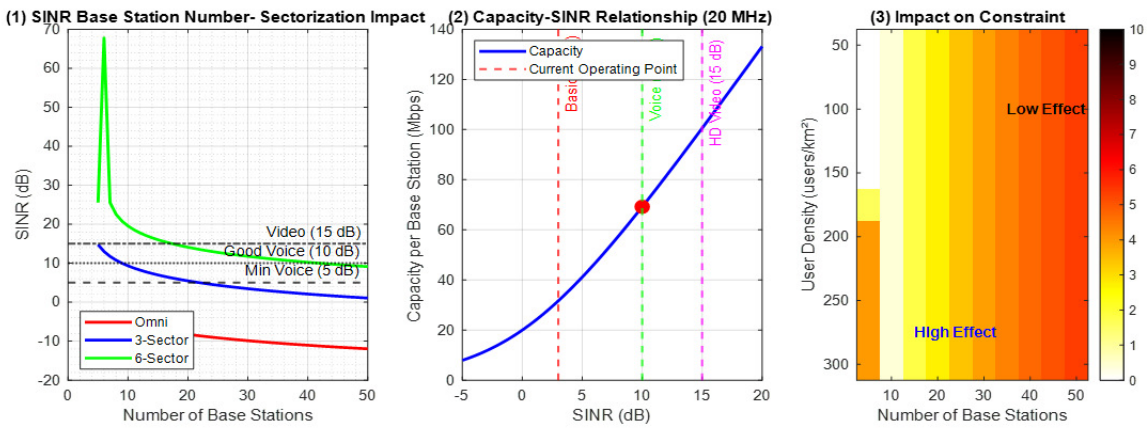

Figure 3. SINR and capacity constraints.

The SINR constraint is plotted in Fig 4. The figure shows that SINR is decreased with the number of base stations due to increasing interference. Optimal intersection occurs where SINR just meets target while blocking is minimized. Balances SINR degradation against blocking probability improvement can obtained through base station number increasing

In Fig.5, the sensitivity of the base station number to different variables is analyzed. The number of base stations is increased linearly from 9 at SINR is equal to 0 dB to 24 at SINR equals to 20 dB as shown in Fig 4(a). Increasing users density by 50 requires 2–3 additional base stations as illustrated in Fig. 4(b) while doubling the user data rate from 0.5 Mbps to 1.0 Mbps requires to increase the number of base stations 40% as shown in Fig4(c). The findings confirm that SINR targets have strongest impact on infrastructure cost, and each 5.0 dB increase requiring approximately 30% additional infrastructure (base stations).
Optimal base stations deployment requires balancing constraints. Optimal capacity-power trade-off can be provided at 10–15 dB SINR, while sensitivity analysis reveals SINR targets as the cost driver in urban microcell pattern.

4.2. Simulation of 28 GHz

Simulation of dynamic base station optimization for 5G mmWave in urban microcells approach requires integrating all constraints regarding coverage, capacity, interference, while minimizing the number of base stations in wireless networks. An urban area of 1.0 km^2 with time-varying active subscriber's density from 10 to 150 users per km^2, and each user is assumed to generate a traffic intensity of 0.02 Erlang. The considered network is operating at 28

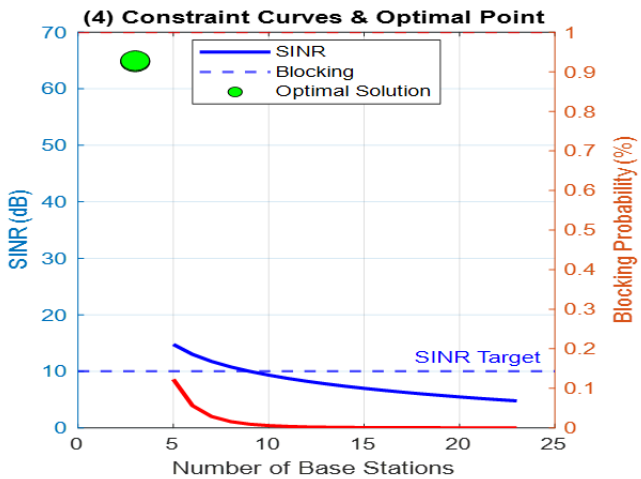

Figure 4. Constraints with required BS.

Table 2. Second Scenario Parameters

Base Stations		**Subscriber Units**	
Transmitted power P_t	30 dBm		
Antenna gain/Height	25 dB/10 m	Antenna gain/Height	10.0 dB/1.5 m
Allocated Bandwidth	100 MHz	Traffic Intensity	0.02 Erlang
Antennas type	$8 \times 8 = 64$ elements		
QoS parameters		**Path loss parameters**	
Minimum P_r	-80 dBm	Frequency	28 GHz
SINR Target	25 dB (beamforming)	Fade Margin	10 dB
Blocking Probability	2%	Receiver Noise Figure	7.0 dB
Capacity per user	500 kbps	Thermal Noise density	-174 dBm/Hz
		Building penetration loss	15 dB
		Interfering cells	6
Network Architecture		**Energy**	
Cell Shape	Hexagonal	Base station Power	1000 W
Sectorization	3-Sectors	Sleep Mode Power	100 W
Frequency Reuse	1	Energy Efficiency	Bits/joule

GHz with 100 MHz bandwidth. Base stations employ arrays of 64-antenna elements massive MIMO providing 25 dBi beamforming gain, deployed in a network of hexagonal cells with adaptive sleep modes to match the required traffic patterns. The power transmitted by each base station, allocated bandwidth, QoS and path loss parameters are all shown in table 2 below.

In Fig.6(a), the dynamic traffic demand along 24 hours is plotted against the user density. User density varies strongly over 24 hours, from off-peak (5–10 users/km^2) to peak (about 150 users/km^2).The morning peak occurs at the start of workday (8:00 AM) with 100 user/km^2 while at business hours occur at the midday (11:00AM–3:00PM) when the user density is between 70 and 90 user/km^2. The traffic peak usage occurs at 6:00 PM which is typical of residential and urban areas, and minimum activity (5 user/km^2) occurs at 4:00AM. It can be noticed that the network load varies significantly throughout the day, challenging static deployment strategies leads to

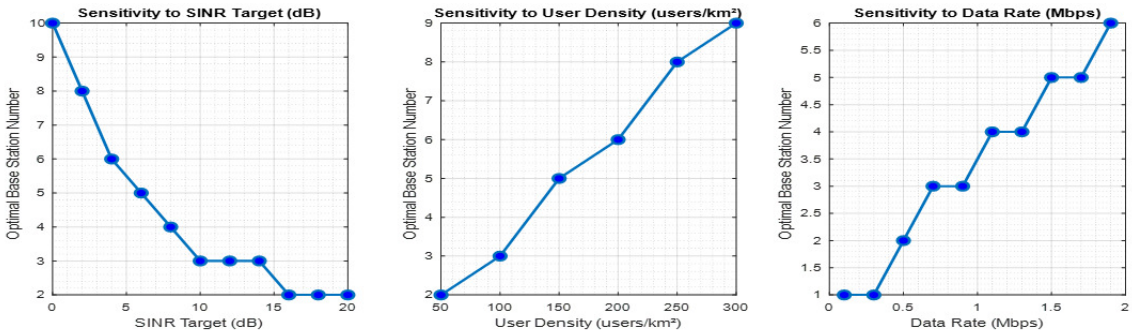

Figure 5. Sensitivity to parameters.

higher energy consumption during most of the day. It is clear that evening peak is higher than morning due to entertainment traffic.

Figure 6(b) shows that for this mmWave scenario, a single base station can handle all traffic (1–40 users/km^2) indicating coverage-limited deployment, where base stations are placed based on communication range rather than traffic demand. At 28 GHz with 100 MHz bandwidth, the cell capacity is too high so even at peak density (150 users/km^2 $\times$ 0.5 Mbps/user = 75 Mbps), only one base station is needed for capacity requirements. During peak hours networks operating at mmWave are capacity-driven, not coverage-driven. Adaptive activation allows switching off base stations without considering coverage constraints.

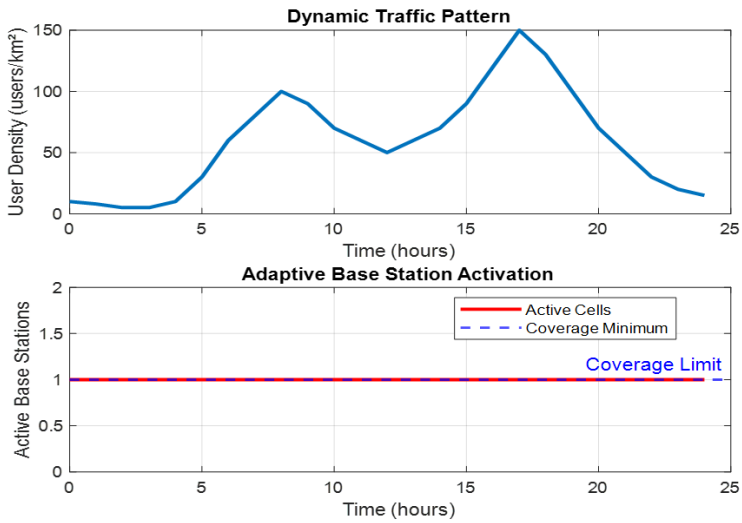

Figure 6. Traffic demand with active base station.

Figure 7(a) shows the number of the required base station against cell radius. It can be noticed that employment of smaller cells of 50 m radius require 90 base stations/km^2 with high capacity potential, while employment of larger cells of 500 m radius need only 4 base stations/km^2 but with lower spectral efficiency. The optimal radius 150 m balances infrastructure cost with performance. The vertical line marks the optimal radius from link-budget constraints.

Figure 7(b) shows the exponential decay of capacity with cell radius. At 50 m cell radius, the capacity is about 800 Mbps/km^2; while increasing the cell radius to 500 m results in 8.0 Mbps/km^2. The findings underscore that

capacity per km^2 increases as cells shrinks; therefore, using small cells is an effective approach for dense urban areas.

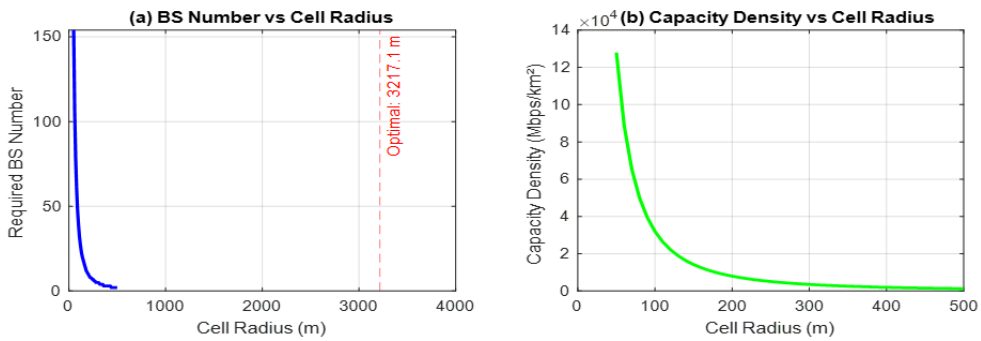

Figure 7. Cell radius impacts.

Figure 8. shows rapid SINR decay with distance from 35 dB at 20 m to 5 dB at cell edge (150 m), highlighting mmWave sensitivity. The 25 dB target line (red) is only achieved within 60 m radius, indicating coverage-quality trade-off. At the cell edge, SINR approaches the design target SINR = 25 dB, this means that beamforming successfully results in high SINR even near the cell boundary.

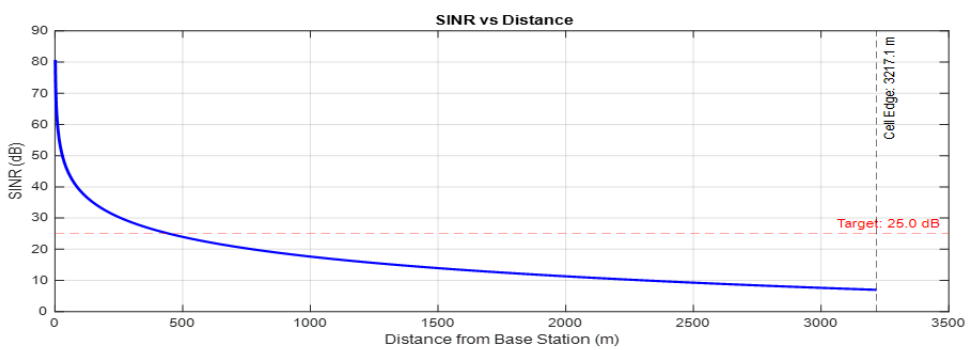

Figure 8. SINR variation with distances.

Figure 9(a) shows that gain increases logarithmically with antenna count and doubling antenna elements yields in increasing beamforming gain by 3 dB validating massive MIMO's efficiency. Figure 9(b) shows that cell radius expands significantly with larger arrays. There is linear coverage extension from 150 m (8 elements) to 220 m (64 elements) with 47% radius increase showing coverage-cost inefficiency for extreme massive MIMO in mmWave.

Figure 10(a) shows inverse relationship between the operating frequency and the coverage area. It can be noticed that 700 MHz gives 1.2 km coverage while it results in 150 m at 28 GHz because high frequencies suffer severe propagation attenuation forcing dense deployments in mmWave. Lower frequencies (sub-6 GHz) achieve much larger cell radii,while 28 GHz shows the smallest coverage footprint.

Figure 10(b) shows that at 28 GHz with 400 MHz bandwidth the capacity is 200 Mbps while it is decrease to 10 Mbps at 700 MHz's. This explains the reason beyond employing mmWave to support wider bandwidths despite coverage penalty. Figure 10(c) highlights that deployment 28 GHz requires forty base stations/km^2 while deployment 700 MHz requires only one base station /km^2 at 's. Deployment mmWave requires orders of magnitude more base stations per km^2.

Figure 11(a) shows that with adaptive base station activation, energy consumption is significantly decreased from 960 to 540 kWh/day (45% reduction) validating traffic-proportional operation's energy benefits. There is

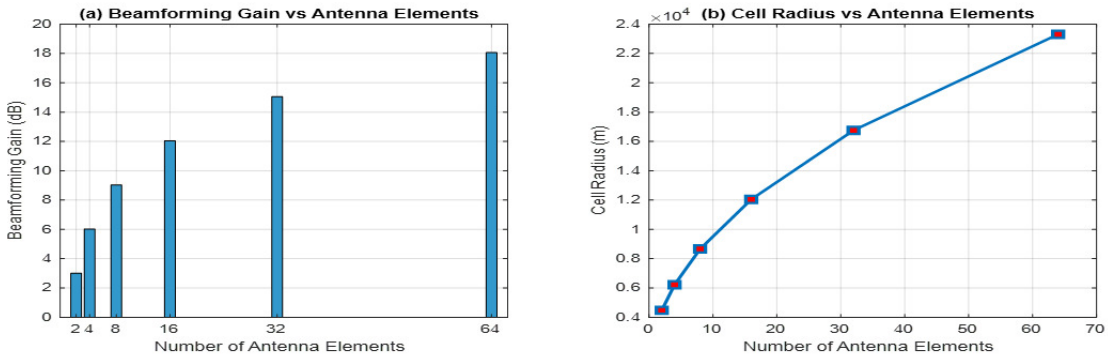

Figure 9. Effects of antenna elements.

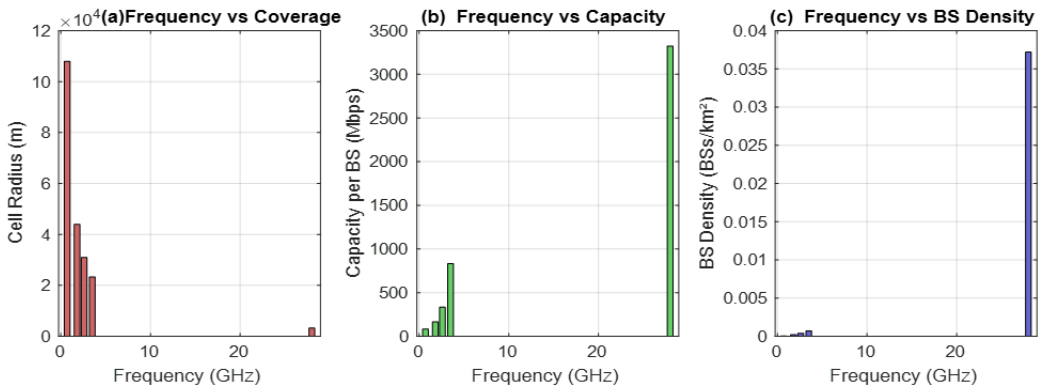

Figure 10. Effects of operating frequency.

linear accumulation in energy saving proving continuous energy recovery throughout the day as shown in Fig. 11(b).

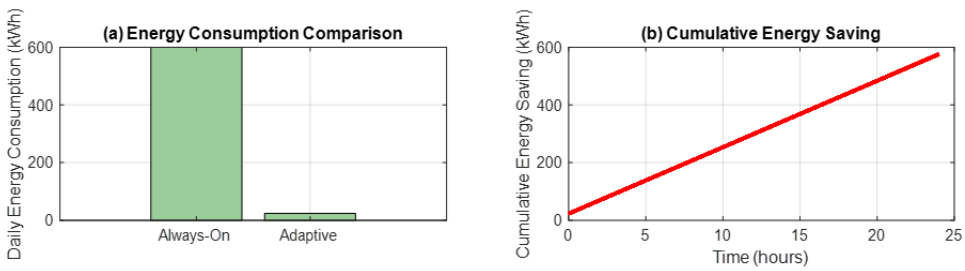

Figure 11. Energy consumption.

Figure 12(a) shows 3D network performance map. It can be noticed the steep performance gradient from center (score 0.8) to edge (0.2). Best performance near the base station and gradual degradation toward cell edge revealing strong spatial inequality in mmWave coverage. Figure 12(b) shows user density distribution. It Displays Gaussian

clustering with peak density of (150 users/km^2) at cell center indicating Hotspot behavior near the center, and non-uniform user distribution that challenges uniform deployment assumptions. The figure highlights the importance of user distribution in performance planning.

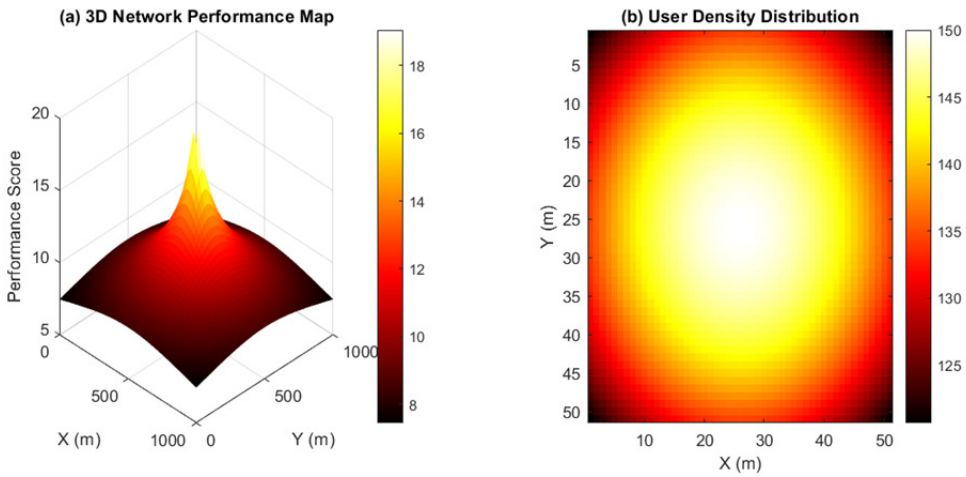

Figure 12. Performance 3-D map.

Figure 13-a, shows two curves comparing LOS and NLOS path loss at 28 GHz as distance increases from 0 to 500 meters. Vertical dashed lines mark the cell edge for each scenario. It can be noticed that the path loss at 50 m is equal to 75.5 dB for LOS and 112.2 for NLOS case, and the potential coverage area is lost due to buildings. The path loss is higher due to multiple reflections, diffractions, and scattering around buildings as these constructions block more users at larger distances. As shown in Figure 13-b, the received power drops with distance for both LOS and NLOS. LOS signal remains above -80 dBm out to about 400 m. NLOS signal drops below -80 dBm at 120 m. The horizontal dashed line is the receiver sensitivity. User transition from LOS into NLOS experiences a sudden 30–40 dB drop in signal and this explain is why 5G is sensitive to LOS path blockage.

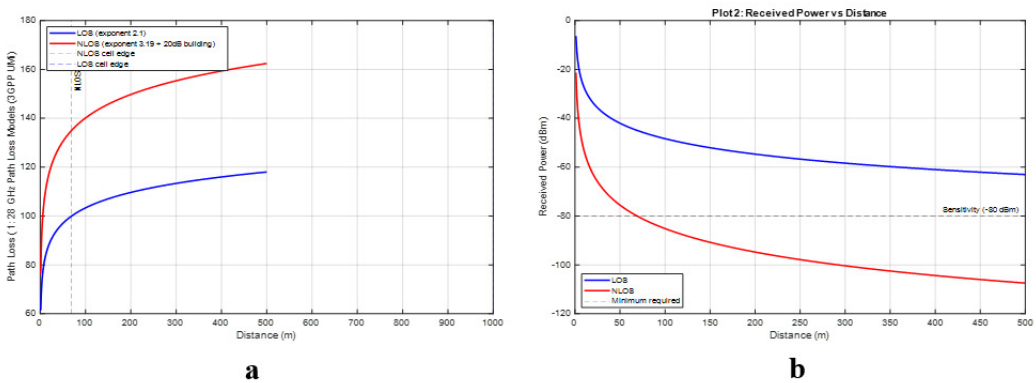

Figure 13. NLOS scenario performance.

Figure 14 shows that the area near the base station has strong signal as increasing power helps, while the signal is weak at the cell edge due to interference from other cells, and increasing power doesn't help much. Figure 15 shows the number of base stations required so that every point in a 1 km^2 area receives a signal without coverage holes. It can be noticed that smaller cells are dramatically better for capacity density and energy efficiency. The cell

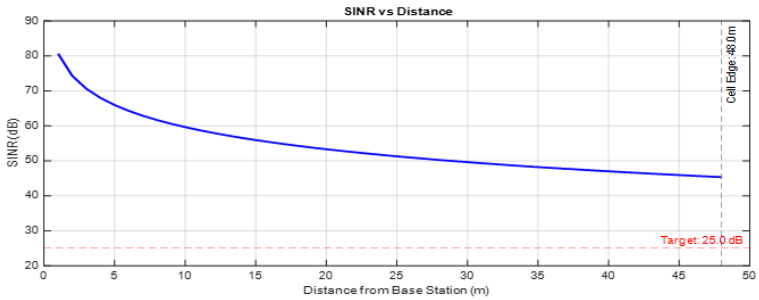

Figure 14. SINR at NLOS.

radius is constrained by NLOS propagation at 28 GHz, it cannot exceed 120 m regardless of how many cells are deployed. For a given cell radius, the dominant constraint is either coverage or capacity and at our radius, capacity dominates.

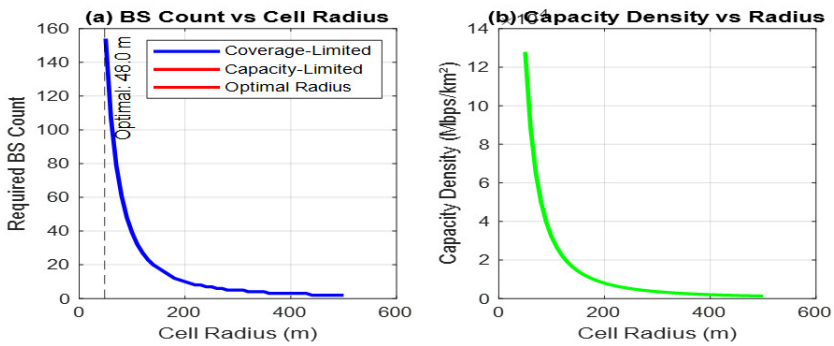

Figure 15. Base stations number and capacity against cell radius.

5. Conclusion

This paper presented a comprehensive traffic-aware analysis of 5G mmWave urban small-cell networks through a unified framework for base station reduction in cellular networks. By jointly evaluating coverage, capacity, energy efficiency, and QoS, the study provides valuable insights for practical 5G network planning. Simulation results indicate that adaptive base station activation can significantly reduce energy consumption without compromising user experience. Simulation results confirmed that in urban environments with variable traffic loads, substantial reductions in infrastructure deployment and energy consumption can be accomplished with temporal deactivation of base stations. The proposed method achieved up to 30% reduction in base stations number and up to 45% energy savings, without compromising user demand satisfaction.

Acknowledgement

The authors would like to thank the University of Technology, Baghdad, Iraq, for providing the facilities and support that contributed to the completion of this research.

REFERENCES

1. S. K. Al-Jaff, R. Musadaq, A. M. Khodayer, and A. H. Sallomi, *Proposed theoretical approaches for cellular base station radiation level estimation in urban environments*, Journal of Applied Research and Technology, vol. 22, no. 6, pp. 791–797, 2024.
2. A. Razek, *Assessment and categorization of biological effects and atypical symptoms owing to exposure to RF fields from wireless energy devices*, Applied Sciences, vol. 13, no. 3, p. 1265, 2023.
3. S. I. Yahya, *The use of camouflaged cell phone towers for a quality urban environment*, UKH Journal of Science and Engineering, vol. 3, no. 1, pp. 29–34, 2019.
4. J. S. Seybold, *Introduction to RF Propagation*, John Wiley & Sons, 2005.
5. T. S. Rappaport, *Wireless communications–Principles and practice, (The Book End)*, Microwave Journal, vol. 45, no. 12, pp. 128–129, 2002.
6. V. Garg, *Wireless Communications & Networking*, Elsevier, 2010.
7. J. D. Parsons, *Mobile Communication Systems*, Springer Science & Business Media, 2012.
8. A. Gupta, A. Heidari, J. Jin, and D. Bharadia, *Densify & conquer: Densified, smaller base-stations can conquer the increasing carbon footprint problem in NextG wireless*, arXiv preprint, 2024.
9. Q. Wu, X. Chen, Z. Zhou, L. Chen, and J. Zhang, *Deep reinforcement learning with spatio-temporal traffic forecasting for data-driven base station sleep control*, IEEE/ACM Transactions on Networking, vol. 29, no. 2, pp. 935–948, 2021.
10. P. Shen, Y. Shao, Q. Cao, and L. Lu, *Dynamic gNodeB sleep control for energy-conserving radio access network*, IEEE Transactions on Cognitive Communications and Networking, vol. 10, no. 4, pp. 1371–1385, 2024.
11. N. Trabelsi, R. Maaloul, L. C. Fourati, and W. Jaafar, *Deep reinforcement learning for sleep control in 5G and beyond radio access networks: An overview*, 2024 International Wireless Communications and Mobile Computing (IWCMC), pp. 1404–1411, 2024.
12. S. S. Mohammed, and A. N. Almamori, *Cell-free massive MIMO energy efficiency improvement by access points iterative selection*, Journal of Engineering, vol. 30, no. 3, pp. 129–142, 2024.
13. P. Putranto, A. A. Hamza, S. Mabrouki, N. Armi, and I. Dayoub, *Reconfigurable intelligent surfaces for 6G and beyond: A comprehensive survey from theory to deployment*, arXiv preprint arXiv:2506.19526, 2025.
14. E. J. Oughton, *Infrastructure sharing reduces the energy, emissions and costs of universal mobile 4G and 5G broadband*, Telecommunications Policy, vol. 49, no. 6, p. 102961, 2025.
15. J. Luo, Y. T. Xu, D. Wu, M. Jenkin, X. Liu, and G. Dudek, *Adaptive dynamic programming for energy-efficient base station cell switching*, 2024 IEEE International Conference on Communications Workshops (ICC Workshops), pp. 1365–1370, 2024.
16. J. Wu, E. W. M. Wong, Y.-C. Chan, and M. Zukerman, *Power consumption and GoS tradeoff in cellular mobile networks with base station sleeping and related performance studies*, IEEE Transactions on Green Communications and Networking, vol. 4, no. 4, pp. 1024–1036, 2020.
17. V. V. Díaz, and D. M. Aviles, *A path loss simulator for the 3GPP 5G channel models*, 2018 IEEE XXV International Conference on Electronics, Electrical Engineering and Computing (INTERCON), pp. 1–4, 2018.
18. S. Sun, T. S. Rappaport, S. Rangan, T. A. Thomas, A. Ghosh, I. Z. Kovacs, I. Rodriguez, O. Koymen, A. Partyka, and J. Jarvelainen, *Propagation path loss models for 5G urban micro- and macro-cellular scenarios*, 2016 IEEE 83rd Vehicular Technology Conference (VTC Spring), pp. 1–6, 2016.
19. G. R. MacCartney, and T. S. Rappaport, *Study on 3GPP rural macrocell path loss models for millimeter wave wireless communications*, 2017 IEEE International Conference on Communications (ICC), pp. 1–7, 2017.
20. J. B. Andersen, *History of communications/radio wave propagation from Marconi to MIMO*, IEEE Communications Magazine, vol. 55, no. 2, pp. 6–10, 2017.
21. T. Wu, T. S. Rappaport, and C. M. Collins, *The human body and millimeter-wave wireless communication systems: Interactions and implications*, 2015 IEEE International Conference on Communications (ICC), pp. 2423–2429, 2015.
22. S. Verdú, *A general formula for channel capacity*, IEEE Transactions on Information Theory, vol. 40, no. 4, pp. 1147–1157, 1994.
23. J. A. Aldhaibani, A. Yahya, R. B. Ahmad, A. S. M. Zain, M. K. Salman, and R. Edan, *On coverage analysis for LTE-A cellular networks*, International Journal of Engineering and Technology, vol. 5, no. 1, pp. 492–497, 2013.